

The electronic structure of Ti_2 and Ti_2^+

Apostolos Kalemos and Aristides Mavridis

Citation: *J. Chem. Phys.* **135**, 134302 (2011); doi: 10.1063/1.3643380

View online: <http://dx.doi.org/10.1063/1.3643380>

View Table of Contents: <http://jcp.aip.org/resource/1/JCPSA6/v135/i13>

Published by the [American Institute of Physics](#).

Related Articles

New view of the ICN A continuum using photoelectron spectroscopy of ICN-
J. Chem. Phys. **136**, 044313 (2012)

The ultraviolet photodissociation of CS₂: The S(1D₂) channel
J. Chem. Phys. **136**, 044310 (2012)

Evolution of metastable state molecules N₂(A³ Σ_u^+) in a nanosecond pulsed discharge: A particle-in-cell/Monte Carlo collisions simulation
Phys. Plasmas **19**, 013505 (2012)

Quantum dynamics of proton migration in H₂O dications: H₂⁺ formation on ultrafast timescales
J. Chem. Phys. **136**, 024320 (2012)

Electronic structure and bonding of HBeLi, HmgLi, and HCaLi in their bent equilibrium geometries
J. Chem. Phys. **136**, 024305 (2012)

Additional information on *J. Chem. Phys.*

Journal Homepage: <http://jcp.aip.org/>

Journal Information: http://jcp.aip.org/about/about_the_journal

Top downloads: http://jcp.aip.org/features/most_downloaded

Information for Authors: <http://jcp.aip.org/authors>

ADVERTISEMENT

**AIP**Advances

Submit Now

**Explore AIP's new
open-access journal**

- **Article-level metrics
now available**
- **Join the conversation!
Rate & comment on articles**

The electronic structure of Ti_2 and Ti_2^+

Apostolos Kalemios^{a)} and Aristides Mavridis^{b)}

National and Kapodistrian University of Athens, Department of Chemistry, Laboratory of Physical Chemistry, Panepistimiopolis – Athens 15771, Hellas

(Received 27 July 2011; accepted 7 September 2011; published online 3 October 2011)

The Ti_2 and Ti_2^+ molecular systems have been studied through multireference variational and single reference coupled-cluster methods coupled with large basis sets. Potential energy curves have been constructed for 30 (Ti_2) and 2 (Ti_2^+) states and the usual spectroscopic parameters have been extracted. The main feature of the potential curves is the existence of van der Waals minima (Ti_2) around 7 bohr irrespective of the molecular symmetry, and $4s^2$ – $4s^1$ interactions (Ti_2^+) around 6 bohr. Numerous avoided crossings lead to stronger covalent bonds emanating from $4s^1$ – $4s^1$ atomic distributions. The X-state of the neutral species is formally a $^3\Delta_g$ state with the first excited state lying within 1 kcal/mol. The removal of the symmetry defining e^- leads to the $X^2\Sigma_g^+$ state of Ti_2^+ .

© 2011 American Institute of Physics. [doi:10.1063/1.3643380]

I. INTRODUCTION

The purpose of the present study is to paint a comprehensive picture on the electronic structure and bonding of the Ti_2 and Ti_2^+ molecules. The severe computational and conceptual difficulties of the $3d$ –transition metal (M) containing compounds and, in particular, of the M_2 systems are well known (Refs. 1 and 2); but see also below.

The first experimental observation on Ti_2 was reported almost half a century ago by Kant and Strauss,³ via a combination of Knudsen equilibrium effusion techniques with mass-spectrometric analysis at high temperatures. By assuming an electronic state of $^1\Sigma$ symmetry, a bond distance twice the Pauling radius of Ti,⁴ and a harmonic frequency 1.25 times the Debye frequency of the element ($\omega = 331 \text{ cm}^{-1}$), an upper limit to the dissociation energy was obtained, $D_0^0 < 52 \text{ kcal/mol}$.³ Five years later, Kant and Lin⁵ assuming as well a $^1\Sigma$ ground state gave a new set of indirectly obtained experimental values: $r_0 = 2.65 \text{ \AA}$, $\omega = 288 \text{ cm}^{-1}$ (using Badger's rule), and $D_0^0 = 28.3 \pm 4$ or $32.8 \pm 5 \text{ kcal/mol}$ depending on the approach followed, i.e., the second or third law, respectively. By considering a $^7\Delta(^7\Sigma)$ ground state the third law D_0^0 value becomes 32.8 ± 5 (36.7 ± 5) kcal/mol.⁵ Using resonance Raman spectroscopy in Ar matrices, Cossé *et al.*⁶ reported the harmonic and anharmonic frequencies of Ti_2 , $\omega_e = 407.9$ and $\omega_e x_e = 1.08 \text{ cm}^{-1}$.

Bier *et al.*⁷ recalculated the dissociation energy of Ti_2 by employing more accurate r_e and ω_e values using the experimental results of Ref. 3. They obtained $D_0^0 = 33.9, 48.4$, or 24.2 kcal/mol depending on the approach used, i.e., the second-law, the third-law, or the Leroy–Bernstein method, respectively, a set of quite different values in conflict also with previously reported D_0^0 results; see also Ref. 8.

Through “mass-resolved resonant two photon ionization spectroscopy in a jet-cooled molecular beam (R2PI),” and assuming a $^3\Delta_g$ ground state as suggested by theoretical

calculations by Bauschlicher *et al.*,⁹ Doverstål *et al.*¹⁰ were able to assign the observed rotational lines as the 0–0 band of the $^3\Pi_{0u} \leftarrow X^3\Delta_{1g}$ transition of Ti_2 . They obtained $r_0(^3\Delta_g) = 1.9422 \pm 0.0008 \text{ \AA}$, $r_0(^3\Pi_u) = 1.997 \pm 0.009 \text{ \AA}$, $\Delta G'_{1/2} = 394.14 \text{ cm}^{-1}$, and $D_0^0 \geq 1.349 \text{ eV}$ ($=31.1 \text{ kcal/mol}$). In addition, based on the latter D_0^0 value and an approximate value of the ionization energy (IE) of Ti_2 , $\text{IE} = 6.125 \text{ eV}$,⁹ they estimated a lower limit of the dissociation energy of Ti_2^+ , $D_0^0 \geq 2.052 \text{ eV}$. This value is consistent with an experimental $D_0^0(\text{Ti}_2^+)$ result of $2.37 \pm 0.07 \text{ eV}$ measured by Armentrout and co-workers.¹¹ In 1991, Russon *et al.*¹² obtained an accurate dissociation energy of Ti_2^+ , $D_0^0 = 2.435 \pm 0.002 \text{ eV}$ ($=56.15 \pm 0.05 \text{ kcal/mol}$). The latter value combined with a better estimate of the ionization energy of Ti_2 , $\text{IE} = 5.93 \pm 0.19 \text{ eV}$,¹² gives $D_0^0(\text{Ti}_2) = 1.54 \pm 0.19 \text{ eV}$ ($=35.5 \pm 4.4 \text{ kcal/mol}$). Three years later Doverstål *et al.*¹³ through the R2PI method extracted spectroscopic parameters for an upper $^3\Delta_u$ state, namely, $r_0 = 2.0425(14) \text{ \AA}$, $T(^3\Delta_u \leftarrow X) = 9092.91(1) \text{ cm}^{-1}$, and $A(\text{spin-orbit constant}) = 38.79 \text{ cm}^{-1}$. Recently, Himmel and Bihlmeier¹⁴ employing UV–visible and resonance Raman spectra of Ti_2 in noble gas matrices, reported $D_e(D_0) = 27.2$ (26.6) kcal/mol, considerably lower than the $35.5 \pm 4.4 \text{ kcal/mol}$ of Russon *et al.*¹² Finally, Hübner *et al.*¹⁵ in a combined experimental (visible absorption spectroscopy)–theoretical work, gave experimental ω_e , $\omega_e x_e$, and T_e values for the upper $1^3\Pi_u$, $1^3\Phi_u$, $2^3\Pi_u$, and $2^3\Phi_u$ states of Ti_2 .

The first non-empirical calculations on the $3d$ – M_2 (M = Sc–Cu) series at the Hartree–Fock level were done by Wolf and Schmidtke,¹⁶ who reported $r_e(X^1\Sigma_g^+) = 1.87 \text{ \AA}$ and $\omega_e = 580 \text{ cm}^{-1}$ for the Ti_2 dimer. A few years later, Walch and Bauschlicher performed multireference configuration interaction (MRCI) calculations on Ti_2 .¹⁷ In 1991, Bauschlicher *et al.*⁹ reinvestigated the Ti_2 molecule; they examined four states $^7\Sigma_u^+$, $^1\Sigma_g^+$, $^3\Delta_g$, and $^3\Sigma_u^+$ by valence MRCI and ACPF (averaged coupled pair functional)/[$6s6p4d2f1g$] methods. Core correlation effects of the $3s^23p^6$ subvalence electrons were estimated through MCPF (modified coupled

^{a)}Electronic mail: kalemios@chem.uoa.gr.

^{b)}Electronic mail: mavridis@chem.uoa.gr.

pair functional)/[8s8p5d2f] and CCI (externally contracted CI)/[8s7p4d1f] techniques. At the valence MRCI and ACPF levels the ground state appears to be of ${}^7\Sigma_u^+$ symmetry, but the inner shell correlation seems to favor a ${}^3\Delta_g$ ground state.⁹

Eight years later, Suzuki *et al.*¹⁸ studied 27 states of Ti_2 of ${}^3\Delta_g$ symmetry by the state-averaged complete active space self consistent field (SA-CASSCF)/[8s5p3d2f – Slater type orbitals] methodology. A potential energy curve (PEC) of the lowest ${}^3\Delta_g$ state was constructed at the MRCI level applying a 0.05 threshold. At the MRCI+Q (Davidson correction) level it was found that $D_e^0 = 0.96$ eV (=22.1 kcal/mol), $r_e = 2.096$ Å, and $\omega_e = 320$ cm⁻¹.

The last *ab initio* work on Ti_2 is that of Hübner *et al.*¹⁵ These workers examined a total of 17 states (3 *gerade* and 14 *ungerade*) at the MRCI/[7s6p4d3f2g] level around equilibrium. For certain states the $3p^6$ subvalence correlation and/or scalar relativistic effects have been taken into account, whereas for the ${}^3\Delta_g$ state a single point calculation has been performed including the $3s^23p^6$ correlation along with relativistic effects. Their results will be contrasted with ours later on. Finally, from 1979 to 2006 a series of eleven articles appeared in the literature based on the density functional theory (DFT),¹⁹ with results varying wildly depending on the functional employed.

It is proper at this point to synopsise the most reliable experimental results on Ti_2 , accepting that the ground state is ${}^3\Delta_g$, although this was never proved definitely either experimentally or theoretically:

$$\begin{aligned} X^3\Delta_g: \quad r_0 &= 1.9422 \pm 0.0008 \text{ \AA}, \text{ (Ref. 10);} \\ D_0^0 &= 35.5 \pm 4.4 \text{ kcal/mol, (Ref. 12),} \\ \omega_e &= 407.9 \text{ cm}^{-1}, \omega_e x_e = 1.08 \text{ cm}^{-1} \text{ (Ref. 6).} \\ \\ {}^3\Pi_u: \quad r_0 &= 1.997 \pm 0.009 \text{ \AA}, \\ \Delta G'_{1/2} &= 394.14 \text{ cm}^{-1} \text{ (Ref. 10).} \\ \\ {}^3\Delta_u: \quad r_0 &= 2.0425(14) \text{ \AA}, T = 9092.91 \text{ cm}^{-1} \text{ (Ref. 13).} \end{aligned}$$

As to the existing literature now on the Ti_2^+ dimer, we are aware of two experimental works^{11,12} both converging to $D_0^0 = 2.435 \pm 0.002$ eV (=56.15 ± 0.05 kcal/mol) and $\text{IE}(\text{Ti}_2) = 5.93 \pm 0.19$ eV (Ref. 12) (*vide supra*). Concerning the ground state of Ti_2^+ it has been suggested to be of ${}^2\Delta_g$ symmetry.¹² Theoretically, there is only a DFT/(BPW91, PW91PW91, BLYP, BPBE) publication on the $3d\text{-M}_2^+$ series, $M = \text{Sc-Zn}$, by Gutsev and Bauschlicher (Ref. 19g).

The above exposition testifies to the necessity for a more thorough examination of the Ti_2 and Ti_2^+ species. To that end we have performed multireference variational and single reference coupled-cluster (CC) calculations for 30 and 2 states of Ti_2 and Ti_2^+ , respectively, using quantitative basis sets. For most states we have constructed complete potential energy curves, reporting energetics and common spectroscopic parameters. It is proper to say at this point, however, that although this is the most extensive and systematic work on Ti_2 so far, our results cannot be deemed as satisfactory due to the egregious problems inherent in the $3d\text{-M}_2$ transition metal dimers.

II. METHODOLOGY

The basis sets employed belong to the correlation consistent family by Balabanov and Peterson,²⁰ namely, the valence cc-pVQZ (=Q ζ) and the corresponding weighted core-valence sets of quadruple cardinality, cc-pwCVQZ (=CQ ζ) both generally contracted to [8s7p5d3f2g1h] and [10s9p7d4f3g2h], respectively. For scalar relativistic Douglas-Kroll-Hess^{21,22} calculations, the cc-pVQZ-DK and cc-pwCVQZ-DK sets were used re-contracted according to Ref. 23.

The calculational methods used are the MRCI (CASSCF + single + double replacements), ACPF (averaged coupled pair functional),²⁴ and RCCSD(T) (restricted coupled-cluster + single + double + perturbative connected triplets).²⁵ All calculations were done under D_{2h} symmetry restrictions. For most states the CASSCF reference wave functions are constructed by distributing the 8 “valence” electrons ($4s^23d^2 \times 2$) to 14 orbitals [(4s + 4p $_z$ + 3d) × 2]. Internally contracted valence (*ic*)MRCI calculations were done through single and double excitations out of the reference spaces.²⁶ Core-valence ($3s^23p^6$) effects at the CI level were unfeasible due to the enormous ensuing spaces. The size of the valence (*ic*)MRCI expansions range from $\sim 4.5 \times 10^6$ (quintets) to 9.5×10^6 (triplets) configuration functions. Size non-extensivity errors estimated to be less than 10 mE $_h$ were accounted for through the Davidson (+Q) correction.²⁷ Four states ${}^3\Delta_g$, ${}^1\Sigma_g^+$, ${}^7\Sigma_u^+$, and ${}^3\Sigma_u^+$ were also examined at the valence and core-valence ($3s^23p^6$) coupled-cluster level of theory, RCCSD(T)/Q ζ , and C-RCCSD(T)/CQ ζ , respectively. Scalar relativity was taken into account through the second order Douglas-Kroll-Hess (DKH2) approximation.^{21,22} All calculations were performed by the MOLPRO program.²⁸

III. THE COMPLEXITY OF THE Ti_2 MOLECULE

Although $3d\text{-M}_2$ dimers are chemically “naïve” systems, that is, diatomic molecules with a rather small number of electrons, the combined orbital and spin angular momenta give rise to incredibly complex electronic molecular distributions defying all current computational methods.^{1,2} The Ti_2 molecule with 8 outer ($4s^23d^2 \times 2$) and 16 subvalence ($3s^23p^6 \times 2$) electrons, is a most characteristic case. For instance, within an energy range of 13 000 cm⁻¹ (=1.612 eV) there are 6 atomic ${}^{2S+1}L$ Ti terms, namely, $a^3F(4s^23d^2)$, $a^5F(4s^13d^3)$, $a^1D(4s^23d^2)$, $a^3P(4s^23d^2)$, $b^3F(4s^13d^3)$, and $a^1G(4s^23d^2)$.²⁹ Starting from the energetically lowest asymptote $a^3F + a^3F$ and up to $a^5F + a^5F$ asymptote there are 7 dissociating channels [$a^3F + (a^3F, a^5F, a^1D, a^3P, b^3F, a^1G)$] resulting overall to 762 (4984) $|\Lambda\Sigma\rangle$ ($|\Omega\rangle$) molecular Ti_2 states, a real challenge for every existing method of solving the eigenvalue Schrödinger equation. Considering that the energy range of molecular Ti_2 states is more-or-less the same with the asymptotic energy range $\Delta E \sim 13\,000$ cm⁻¹, the mean energy separation per state is $\sim 13\,000/762 = 17$ ($|\Lambda\Sigma\rangle$) or $13\,000/4984 = 2.6$ ($|\Omega\rangle$) cm⁻¹. The symmetries of all 762 $|\Lambda\Sigma\rangle$ states resulting from the 7 channels, $a^3F + a^3F \rightarrow a^5F + a^5F$, are (singlets to nonets)^{1,3,5,7,9} ($\Sigma^\pm, \Pi, \Delta, \Phi, \Gamma, H, I, K$) $_{g,u}$. Therefore, it is obvious that obtaining either experimental or theoretical

TABLE I. Energies $E(E_h)$, bond distances $r_e(\text{\AA})$, dissociation energies $D_e(\text{kcal/mol})$, harmonic and anharmonic frequencies ω_e , $\omega_e x_e(\text{cm}^{-1})$, and energy separations $T_e(\text{kcal/mol})$ of the first four states of Ti_2 .

State	Method ^a	-E	r_e	D_e^b	ω_e	$\omega_e x_e$	T_e
$X^3\Delta_g$	MRCI+Q	1696.957 09	2.009	18.4	369	1.70	
	ACPF	1696.955 50	2.008	19.2	370	2.37	
	RCCSD(T)	1696.951 81	1.976	15.8	401	4.58	
	MRCI-DKH2+Q	1705.619 97	2.019	14.6	366	1.11	
	ACPF-DKH2	1705.618 36	2.018	14.4	367	1.95	
	RCCSD(T)-DKH2	1705.613 50	1.965	10.7	437	0.89	
	C-RCCSD(T)	1697.738 43	1.899	30.6	495	1.32	
	C-RCCSD(T)-DKH2	1706.400 30	1.907	26.1	490	1.25	
	Ref. 15 ^c		1.954	37.1	432		
	Expt.		1.9422 ^d	35.5±4.4 ^e	407.9 ^f	1.08 ^f	
$1^1\Sigma_g^+$	MRCI+Q	1696.955 34	2.017	17.3	431	3.33	1.10
	ACPF	1696.953 30	2.023	17.8	416	1.56	1.38
	RCCSD(T)	1696.950 32	2.002	14.8	449	2.24	0.94
	MRCI-DKH2+Q	1705.618 37	2.025	13.6	423	1.20	1.01
	ACPF-DKH2	1705.617 27	2.028	13.7	416	1.53	0.68
	RCCSD(T)-DKH2	1705.616 53	2.012	12.6	441	1.19	-1.90
	C-RCCSD(T)	1697.736 11	1.938	29.2	513	-3.96	1.45
	C-RCCSD(T)-DKH2	1706.401 18	1.956	26.6	494	1.04	-0.56
	Ref. 15 ^g		2.023		422		0.92
	Ref. 15 ^h		1.968		479		3.92
$2^7\Sigma_u^+$	MRCI+Q	1696.955 58	2.578	40.3	207	0.42	0.95
	ACPF	1696.952 98	2.581	40.0	203	0.59	1.59
	MRCI-DKH2+Q	1705.623 37	2.556	41.8	214	0.52	-0.60
	ACPF-DKH2	1705.619 64	2.561	41.0	210	0.63	-0.80
	Ref. 15 ⁱ		2.446		244		7.15
$3^3\Sigma_u^+$	MRCI+Q	1696.948 23	2.155	12.8	2645	0.48	5.56
	ACPF	1696.946 53	2.152	13.5	264	0.27	5.63
	RCCSD(T)	1696.940 62	2.093	8.8	269	-1.59	7.02
	MRCI-DKH2+Q	1705.616 37	2.162	12.3	278	0.93	2.26
	ACPF-DKH2	1705.614 64	2.159	12.1	278	0.87	2.33
	RCCSD(T)-DKH2	1705.608 35	2.116	7.4	306	0.16	3.23
	C-RCCSD(T)	1697.719 11	1.996	18.5			12.12
	C-RCCSD(T)-DKH2	1706.385 52	2.029	16.8	341	-1.44	9.27
	Ref. 15 ^g		2.169		257		2.08
	Ref. 15 ^h		2.051		315		11.53

^a+Q, DKH2, and C - refers to the Davidson correction, scalar relativity, and core ($3s^23p^6$) correlation, respectively.

^bWith respect to the adiabatic fragments $a^3F + a^3F$ ($X^3\Delta_g$, $1^1\Sigma_g^+$, $3^3\Sigma_u^+$) and $a^3F + a^5F$ ($2^7\Sigma_u^+$).

^cC-MRCI + scalar relativity (s.r.) + Q (based on configurations (CF) whose weight at the CASSCF level is larger than 0.01).

^dReference 10.

^eReference 12, D_0 value.

^fReference 6.

^gMRCI + s.r. + Q.

^hC-MRCI + Q (CFs > 0.01, $3p^6 e^-$ included).

ⁱC-MRCI + s.r. + Q (CFs > 0.01, $3p^6 e^-$ included).

reliable results for a Ti_2 -like system is an arduous task indeed. Even the concept of the ground state seems to lose its physical meaning in an almost continuous manifold of states.

Presently, we have constructed PECs for 30 states at the MRCI+Q/Q ζ level, 10 singlets ($^1(\Sigma_g^+[2], \Pi_u, \Pi_g, \Delta_g[2], \Phi_g[2], \Phi_u, \Gamma_g)$), 13 triplets ($^3(\Sigma_u^+, \Sigma_g^-[2], \Pi_g[2], \Pi_u[2], \Delta_g, \Phi_g, \Phi_u[2], \Gamma_g, H_u)$), 6 quintets ($^5(\Pi_u, \Pi_g[2], \Phi_g[2], H_g)$), and one septet ($^7\Sigma_u^+$). We have calculated as well two doublets ($^2(\Sigma_g^+, \Delta_g)$) for the Ti_2^+ cation.

All examined states but the $^7\Sigma_u^+$ correlate adiabatically to the ground state atoms ($a^3F + a^3F$), whereas the $^7\Sigma_u^+$ correlates to $a^3F + a^5F$. It is interesting to mention that the two lowest and practically degenerate states according to the present work, $^3\Delta_g$ and $1^1\Sigma_g^+$, correlate diabatically to two excited a^5F Ti atoms (*vide infra*).

IV. RESULTS AND DISCUSSION

A. Ti_2

Table I lists numerical results of the first four states of Ti_2 in a variety of methods, whereas Table II collects results for 26 higher states at the MRCI+Q/Q ζ level; Figures 1 and 2 display MRCI+Q/Q ζ PECs and a relative energy level diagram of the 30 states presently examined. Between “infinity” (=12 bohr) and the repulsive part of the PECs we can distinguish three interacting regions: a van der Waals (vdW) around 7.0 b, a very “messy” one between 7 and 5 b, and the equilibrium region between 4.7 and 3.6 b. The vdW PECs originate from the $a^3F(4s^23d^2) + a^3F(4s^23d^2)$ channel, with interactions ranging from 8.0 ($^1\Gamma_g$) to 4.0 ($^3\Sigma_g^-$) mE_h . The number of vdW states shown in Figure 1 is 24 (12 singlets, 6 triplets,

TABLE II. Bond distances r_e (Å), dissociation energies D_e (kcal/mol), harmonic frequencies ω_e (cm⁻¹), and energy separations T_e (kcal/mol) of 26 higher states of Ti₂ at the MRCI+Q/Q ζ level of theory.

State	r_e	D_e^a	ω_e	T_e
4 ¹ Δ_g	1.977	11.8[55.1] ^b	364	6.62
Ref. 15 ^c	2.006		356	7.38
Ref. 15 ^d	1.930		432	7.84
5 ⁵ Π_u	2.143	9.9[53.2] ^b	278	8.47
Ref. 15 ^c	2.148		283	7.84
Ref. 15 ^d	2.036		343	10.38
6 ³ Π_u	2.124	8.3[51.6] ^b	326	10.08
Ref. 15 ^c	2.122		330	9.69
Ref. 15 ^c	2.127		333	9.46
Expt. (Ref. 15)	2.032 ^f		371.5	11.53
Expt. (Ref. 10)	1.997±0.009		394.14 (=Δ <i>G</i> _{1/2})	
7 ³ Φ_u	2.133	7.7[51.0] ^b	313	10.69
Ref. 15 ^e	2.131		317	10.15
Ref. 15 ^c	2.136		320	9.92
Expt. (Ref. 15)	2.042 ^f		359.5	12.45
8 ⁵ Π_g	2.362	6.1[28.9] ^g	232	11.83
9 ⁵ Φ_g	2.370	5.6[28.4] ^g	240	12.32
10 ³ Π_g	2.413	4.9[27.2] ^g	203	13.50
11 ³ Φ_g	2.421	4.2[26.5] ^g		14.21
12 ³ Π_g	2.330	2.8[25.2] ^g		15.57
13 ¹ Π_g	2.364	2.7[35.8] ^h	264	15.67
14 ¹ Φ_g	2.512	1.8[34.9] ^h		16.62
15 ³ H_u	2.224	1.8[45.1] ^b	228	16.62
Ref. 15 ^c	2.220		230	16.14
Ref. 15 ^c	2.225		244	15.91
16 ¹ Φ_u	2.140	0.87[44.2] ^b	328	17.51
17 ³ Π_u	2.184	0.74[44.1] ^b	259	17.64
Ref. 15 ^c	2.184		259	17.07
Ref. 15 ^c	2.191		270	16.83
Expt. (Ref. 15)	2.072 ^f		282	20.30
18 ⁵ Π_g	2.342	[22.8] ^g	277	17.96
19 ⁵ Φ_g	2.324	[22.4] ^g	274	18.38
20 ⁵ H_g	2.358	[22.3] ^g	259	18.40
21 ³ Σ_g^-	2.320	[42.6] ^b	266	19.07
	1.973		296	
22 ¹ Γ_g	2.084	[42.1] ^b	183	19.58
23 ¹ Φ_g	2.516	[31.6] ^h		19.90
24 ³ Γ_g	2.327	[41.5] ^b	265	20.16
25 ¹ Σ_g^+	2.075	[41.5] ^b	184	20.24
26 ¹ Π_u	2.176	[40.6] ^b	279	21.05
27 ³ Σ_g^-	2.172	[40.6] ^b	480	21.07
28 ³ Φ_u	2.185	[39.2] ^b	261	22.46
Ref. 15 ^c	2.179		268	21.91
Ref. 15 ^c	2.186		278	21.68
Expt. (Ref. 15)	2.072 ^f		288	23.75
29 ¹ Δ_g	2.416	[35.7] ^b	238	26.02

^aWith respect to adiabatic (a³F + a³F) ground state [diabatic] atoms.

^bWith respect to diabatic atoms a³F + a⁵F.

^cMRCI + s.r. + Q.

^dC-MRCI + Q.

^eMRCI+Q.

^f r_e values are calculated indirectly by the present authors according to the relation $r_e = r_e(X^3\Delta_g)^{10} + \Delta r_e$, where Δr_e are experimentally determined values in Ref. 15.

^gWith respect to diabatic atoms a³F + a⁵F.

^hWith respect to diabatic atoms a³F + b³F.

ⁱThe 21³ Σ_g^- features two minima, a global, and a local.

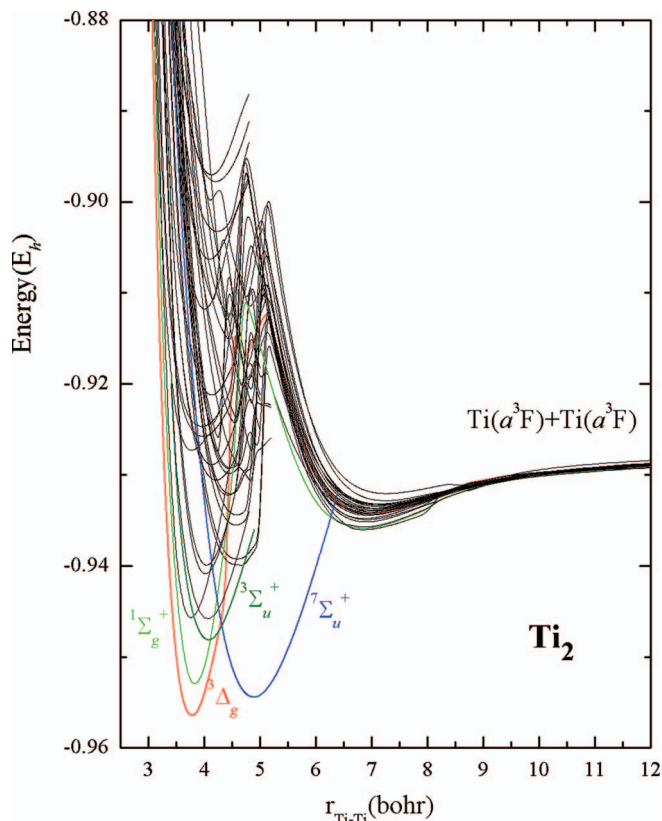


FIG. 1. MRCI+Q/Q ζ PECs of 30 states of Ti₂. Energies have been shifted by +1696.0 E_h.

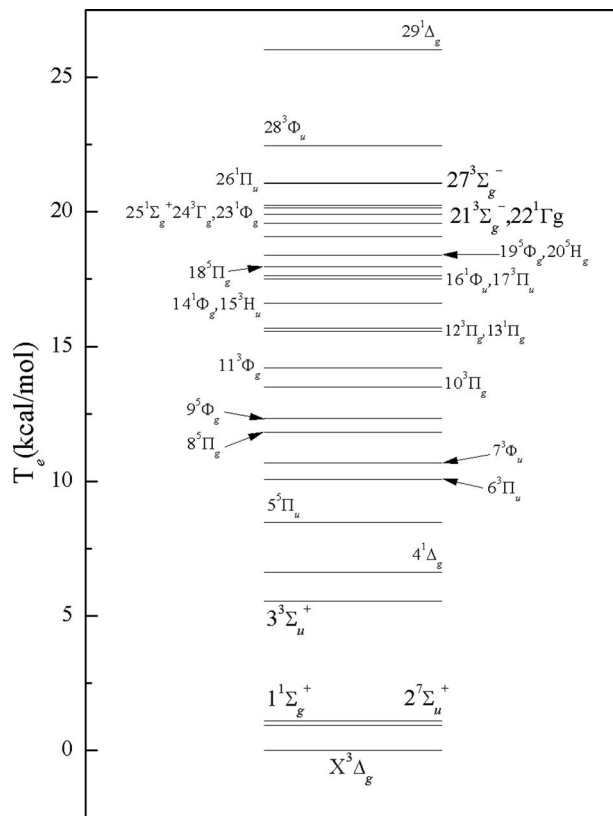


FIG. 2. Relative energy level diagram of Ti₂ of 30 states at the MRCI+Q/Q ζ level.

6 quintets), out of a possible 84 $|\Lambda\Sigma\rangle$ states correlating to $a^3F + a^3F$ Ti atoms. Certainly, all 84 states would show similar vdW interactions and minima close to 7 b, approximately twice the $\{3d^2(^3F)\}4s^2$ atomic Ti radius of ~ 3.8 b.³⁰

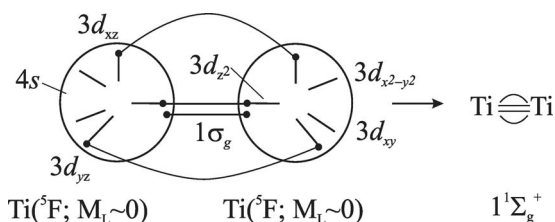
The “messy” region between 7 and 5 b is the result of numerous avoided crossings of the repulsive part of the vdW PECs, with incoming strongly attractive PECs of the same symmetry emanating from higher channels; see Figure 1. We turn now to the discussion of the first four states of Ti₂.

1. $X^3\Delta_g$, $1^1\Sigma_g^+$, $2^7\Sigma_u^+$, and $3^3\Sigma_u^+$

As was already discussed two ground state (a^3F) Ti atoms lead only to non-covalent $4s^2-4s^2$ vdW interactions. Attractive interactions are expected from higher channels, e.g., $4s^23d^2(a^3F)-4s^13d^3(a^5F, b^3F)$ and $4s^13d^3(a^5F)-4s^13d^3(a^5F)$. The first two, practically degenerate states according to our calculations (*vide infra*), $X^3\Delta_g$ and $1^1\Sigma_g^+$, correlate diabatically to two a^5F Ti atoms, whereas the next two states, $2^7\Sigma_u^+$ and $3^3\Sigma_u^+$, are related to $a^3F + a^5F$ atoms. The leading equilibrium CASSCF configurations and corresponding Mulliken densities of the first two states are (valence electrons only)

$$\begin{aligned} |X^3\Delta_g\rangle &\approx 0.86|1\sigma_g^2 2\sigma_g^1 1\pi_{x,u}^2 1\pi_{y,u}^2 1\delta_g^1\rangle \\ &\quad 4s^{0.99} 4p_z^{0.02} 3d_{z^2}^{0.49} 4p_x^{0.06} 4p_y^{0.06} 3d_{xz}^{0.92} 3d_{yz}^{0.92} 3d_{\delta}^{0.50} \\ |1^1\Sigma_g^+\rangle &\approx 0.81|1\sigma_g^2 2\sigma_g^1 1\pi_{x,u}^2 1\pi_{y,u}^2\rangle \\ &\quad 4s^{0.99} 4p_z^{0.10} 3d_{z^2}^{0.88} 4p_x^{0.07} 4p_y^{0.07} 3d_{xz}^{0.90} 3d_{yz}^{0.90}. \end{aligned}$$

Taking into consideration that the ratio of the $4s$ and $3d$ radii is $\langle 4s \rangle / \langle 3d \rangle = 2.6$,³⁰ the bonding of the $1^1\Sigma_g^+$ state is captured by the following valence-bond-Lewis (vbL) icon:



The diagram above suggests four bonds, two σ ($1\sigma_g, 2\sigma_g$) and two π ($1\pi_{x,u}, 1\pi_{y,u}$). However, the two π ($3d_{\pi}-3d_{\pi}$) and the one σ ($3d_{z^2}-3d_{z^2}$) singlet coupled distributions are energetically ineffective due to miniscule overlaps. In the $X^3\Delta_g$ state the bonding can be represented with a similar vbL diagram, the difference being the transfer of a $3d_{z^2}-3d_{z^2}(2\sigma_g)$ electron to a δ_g distribution. This bonding similarity between the $X^3\Delta_g$ and $1^1\Sigma_g^+$ states is reflected to the same bond distances and bond energies (Table I).

Despite the extensive size of the present calculations our numerical results are not, in general, very satisfactory indicating the inherent difficulties of the $3d-M_2$ systems. At the valence level the MRCI+Q (ACPF) [RCCSD(T)] bond length is $r_e = 2.009$ (2.008) [1.976] Å; including scalar relativity r_e changes by $\delta r_e = 0.01$ (0.01) [-0.01] Å, respectively. Calculating the correlation of the $3s^23p^6$ subvalence electrons at the MRCI level was proved unfeasible due to the enormous size of the ensuing expansions. Core effects at the RCCSD(T) level (C-RCCSD(T)) decrease the bond length by $\delta r_e = 0.077$ Å. Assuming transferability of core effects

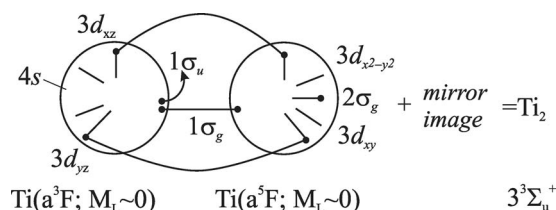
we obtain $r_e = 2.019$ (MRCI-DKH2+Q) - 0.077 (δr_e) = 1.942 Å, identical to the experimental value (Table I). At the C-RCCSD(T)-DKH2 level, however, r_e is predicted shorter by 0.035 Å than the experimental value. Following the same reasoning, the dissociation energy with respect to the ground state atoms is estimated to be $D_e^0 = D_e^0$ (MRCI-DKH2+Q) + $[D_e^0$ (C-RCCSD(T))- D_e^0 (RCCSD(T))] = 14.6 + [30.6-15.8] = 29.4 kcal/mol vs 26.1 kcal/mol at the C-RCCSD(T)-DKH2 level, considerably smaller than the experimental value of 35.5 ± 4.4 kcal/mol.¹² With respect to the $a^5F + a^5F$ diabatic fragments, $D_e = 61.7$ (64.3) [64.8] kcal/mol at the MRCI+Q (MRCI-DKH2+Q) [C-RCCSD(T)-DKH2] level. It is worth mentioning at this point that scalar relativistic effects at all methods reduce the binding energy by 4-5 kcal/mol, while core effects increase the binding energy by the surprising amount of 15 kcal/mol.

For the $1^1\Sigma_g^+$ state scalar relativistic and core effects show the same trends as in the $X^3\Delta_g$ state: the former reduce (increase) the binding energy (bond length) by 2-4 kcal/mol (~ 0.01 Å), while the latter increase the binding energy by 14 kcal/mol, decreasing at the same time the bond distances by 0.064 Å; see Table I. Following the same line of thinking as before, we obtain $r_e = r_e$ (MRCI-DKH2+Q) + $\delta r_e = 2.025-0.064 = 1.961$ Å, and $D_e^0 = D_e^0$ (MRCI-DKH2+Q) + $[D_e^0$ (C-RCCSD(T))- D_e^0 (RCCSD(T))] = 13.6 + [29.2-14.8] = 28.0 kcal/mol as compared to 26.6 kcal/mol at the C-RCCSD(T)-DKH2 level, very similar to the D_e^0 of the $X^3\Delta_g$ state. This means that the $X^3\Delta_g$ and $1^1\Sigma_g^+$ states are degenerate within 1 kcal/mol. This energy separation $T_e = 0.0 \pm 1$ kcal/mol is corroborated at all levels of theory presently employed. As a matter of fact at the C-RCCSD(T)-DKH2 level, the $1^1\Sigma_g^+$ state becomes the ground state by ~ 1 kcal/mol; see Table I.

The main equilibrium CASSCF configurations and Mulliken populations of the next two states are

$$\begin{aligned} |2^7\Sigma_u^+\rangle &\approx |1\sigma_g^2 2\sigma_g^1 1\sigma_u^1 1\pi_{x,u}^1 1\pi_{y,u}^1 [(0.72)1\delta_g^2 - (0.45)1\delta_u^2]\rangle \\ &\quad 4s^{1.25} 4p_z^{0.25} 3d_{z^2}^{0.50} 4p_x^{0.05} 4p_y^{0.05} 3d_{xz}^{0.45} 3d_{yz}^{0.45} 3d_{x^2-y^2}^{0.50} 3d_{xy}^{0.50} \\ |3^3\Sigma_u^+\rangle &\approx 0.87|1\sigma_g^2 2\sigma_g^1 1\sigma_u^1 1\pi_{x,u}^2 1\pi_{y,u}^2\rangle \\ &\quad 4s^{1.31} 4p_z^{0.22} 3d_{z^2}^{0.50} 4p_x^{0.05} 4p_y^{0.05} 3d_{xz}^{0.92} 3d_{yz}^{0.92}. \end{aligned}$$

The $3^3\Sigma_u^+$ correlates diabatically (adiabatically) to the mixed channel $a^3F + a^5F$ ($a^3F + a^3F$), while the $2^7\Sigma_u^+$ dissociates uniquely to $a^3F + a^5F$. The bonding in the $3^3\Sigma_u^+$ state can be captured by the vbL diagram below:



The bonding comprises three bonds, two formal ineffective π ($3d_{\pi}-3d_{\pi}$) and one strong σ ($1\sigma_g$) ($4s-4s$), and two electrons coupled into a triplet are distributed to $2\sigma_g \approx 0.96[3d_{z^2}-3d_{z^2}]$ and $1\sigma_u \approx 0.70[4s-4s] - 0.37[4p_z-4p_z]$ orbitals.

By uncoupling the two π_u bonds and distributing the four electrons coupled into a quintet to the four singly occupied $1\delta_g$ and $1\delta_u$ orbitals, the $2^7\Sigma_u^+$ state is obtained, bound through a single σ ($1\sigma_g^2$) bond. This bonding description is in complete conformity with the main equilibrium configurations and the population analysis given above.

There are no experimental results for the $2^7\Sigma_u^+$ and $3^3\Sigma_u^+$ states. According to Table I at the valence level the MRCI–DKH2+Q (ACPF–DKH2) bond distance of the $2^7\Sigma_u^+$ state is 2.556 (2.561) Å, with a $T_e = 0.0 \pm 1$ kcal/mol. However, the results of Ref. 15 suggest that including the $3p^6$ subvalence electrons at the MRCI + scalar relativity + Q level reduces the bond distance by ~ 0.1 Å and increases T_e by 7–8 kcal/mol. Including the $3s^2 3p^6 e^-$ at the C–RCCSD(T) level, our results indicate similar trends with those of Ref. 15, i.e., a reduction of bond length and a considerable increase of the $T_e(2^7\Sigma_u^+ - ^3\Delta_g)$ gap, although the severe multireference character of the $2^7\Sigma_u^+$ state (*vide supra*) does not allow for quantitative conclusions at the C–RCCSD(T) level. Nevertheless, it is rather safe to conclude that the $2^7\Sigma_u^+$ state is separated from the first two states by some 5–10 kcal/mol with a recommended $r_e = 2.45$ Å.

In the $3^3\Sigma_u^+$ state the MRCI–DKH2+Q (ACPF–DKH2) [RCCSD(T)–DKH2], $r_e = 2.162$ (2.159) [2.116] Å and $T_e = 2.26$ (2.33) [3.23] kcal/mol. Correcting the MRCI–DKH2+Q results for core-correlation effects obtained at the CC level, $\delta r_e = -0.097$ Å and $\delta T_e = +5.1$ kcal/mol, we get $r_e = 2.162 - 0.097 = 2.065$ Å and $T_e = 2.26 + 5.1 = 7.4$ kcal/mol, as contrasted to 2.029 Å and 9.27 kcal/mol at the C–RCCSD(T)–DKH2 level of theory: r_e and T_e values by Hübner *et al.*¹⁵ are comparable with the present calculations; see Table I.

2. Higher states

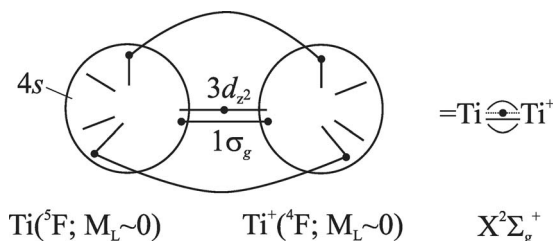
Table II collects r_e , D_e , ω_e , and T_e values of 26 higher states of Ti_2 calculated at the MRCI+Q/Q ζ level and within an energy range of less than 20 kcal/mol. Observe that all states are strongly bound with respect to their diabatic channels, whereas about half of them are also bound with respect to the ground state atoms. According to the results of the first four states previously discussed, core ($3s^2 3p^6$) effects reduce uniformly the bond lengths by 0.10 ± 0.01 Å; see also Ref. 2. In addition, although core effects are of importance to the T_e separations for the first four states, their influence seems to diminish for the higher states as is evidenced from the results of Ref. 15 and the limited experimental values; see Table II. Therefore, we can claim with some confidence that MRCI+Q bond distances should be very close to reality if reduced by about 0.10 Å; on the other hand T_e separations can be considered of a semi-quantitative value. This is corroborated by contrasting theoretical and existing experimental values (in parenthesis) of r_e (after reduction by 0.10 Å) and T_e for the $6^3\Pi_u$, $7^3\Phi_u$, $17^3\Pi_u$, and $28^3\Phi_u$ states: $r_e = 2.02$ (2.00), 2.03(2.04), 2.08(2.07), 2.08(2.07) Å and $T_e = 10.1$ (11.5), 10.7(12.4), 17.6(20.3), 22.5(23.7) kcal/mol, respectively; see Table II.

B. Ti_2^+

We return now to the vbL diagram of the neutral Ti_2 $1^1\Sigma_g^+$ state, practically degenerate to the $X^3\Delta_g$. By removing one electron from the $2\sigma_g(3d_{z^2} - 3d_{z^2})$ orbital the $2^2\Sigma_g^+$ state obtains, while by removing one electron from the $2\sigma_g$ orbital and transferring the other to a $3d_\delta$ atomic distribution, we get a $2^2\Delta_g$ state of Ti_2^+ . The decongestion of the σ frame of Ti_2 by removing one electron and the resulting stabilization of the one electron $2\sigma_g$ bond suggests that the ground state of Ti_2^+ is $2^2\Sigma_g^+$. Indeed, preliminary MRCI calculations indicate that the ground state of Ti_2^+ is of $2^2\Sigma_g^+$ symmetry. Table III lists numerical results for the $2^2\Sigma_g^+$ and $2^2\Delta_g$ states, and Figure 3 displays the corresponding PECs. The main MRCI equilibrium configurations and Mulliken populations of the $X^2\Sigma_g^+$ and $2^2\Delta_g$ states are given below:

$$\begin{aligned} |X^2\Sigma_g^+ \rangle &\approx 0.85 | 1\sigma_g^2 2\sigma_g^1 1\pi_{x,u}^2 1\pi_{y,u}^2 \rangle \\ &\quad 4s^{0.93} 4p_z^{0.04} 3d_{z^2}^{0.50} 4p_x^{0.05} 4p_y^{0.05} 3d_{xz}^{0.93} 3d_{yz}^{0.93} \\ |2^2\Delta_g \rangle &\approx 0.84 | 1\sigma_g^2 1\pi_{x,u}^2 1\pi_{y,u}^2 1\delta_g^1 \rangle \\ &\quad 4s^{0.54} 4p_z^{0.06} 3d_{z^2}^{0.44} 4p_x^{0.03} 4p_y^{0.03} 3d_{xz}^{0.94} 3d_{yz}^{0.94} 3d_{x^2-y^2}^{0.50} \end{aligned}$$

The bonding of the X-state is captured by the following vbL diagram:



As in the $X^3\Delta_g$ state of the neutral species, the bonding comprises of a strong σ bond ($1\sigma_g \sim 4s+4s$) a weak half σ bond ($2\sigma_g \sim 3d_\sigma+3d_\sigma$), and two π ($1\pi_{x,u}$, $1\pi_{y,u}$) weak bonds. By moving the $2\sigma_g$ single electron to a $3d_\delta$ orbital, the $2^2\Delta_g$ is formed some 5 kcal/mol above the $X^2\Sigma_g^+$ state. Both states correlate adiabatically to the ground state fragments $a^3F(4s^2 3d^2) + a^4F(4s^1 3d^2)$.

Following the MRCI PECs from infinity towards equilibrium, a first (local) minimum is observed at 3.3 Å for both states due to a $4s^2(^3F) - 4s^1(^4F)$ interaction, amounting to a 2 center–3 electron bonding of 30 kcal/mol (see Figure 3); see also Ref. 2. Moving to the left and after the avoided crossing with states coming from $Ti(^6F) + Ti^+(^4F)$, the global minima of the $X^2\Sigma_g^+$ and $2^2\Delta_g$ are reached at 2.10 and 1.85 Å, respectively. Observe that between the local (3.30 Å) and global (1.85 Å) minima of the $2^2\Delta_g$ state, there is a middle minimum (2.44 Å) practically isoenergetic to the global one at the MRCI+Q level.

Let us examine now our numerical results listed in Table III. The C–RCCSD(T)–DKH2 binding energy is $D_e(D_0) = 53.2$ (52.7) kcal/mol, in fair agreement with the experimental value $D_0^0 = 56.2 \pm 0.05$ kcal/mol.¹² At the valence MRCI–DKH2+Q (ACPF–DKH2) the binding energy is 47.1 (46.8) kcal/mol. Adding core $3s^2 3p^6$ effects

TABLE III. Energies $E(E_h)$, bond distances $r_e(\text{\AA})$, dissociation energies $D_e(\text{kcal/mol})$, harmonic and anharmonic frequencies ω_e , $\omega_e x_e(\text{cm}^{-1})$, and energy separations $T_e(\text{kcal/mol})$ of the first two states of Ti_2^+ .

State	Method	$-E$	r_e	D_e	ω_e	$\omega_e x_e$	T_e
$X^2\Sigma_g^+$	MRCI+Q	1696.759 75	2.135	47.5	258	0.280	0.0
	ACPF	1696.758 07	2.130	46.9	260	0.292	0.0
	RCCSD(T)	1696.750 07	2.077	42.4	296	-0.210	0.0
	MRCI-DKH2+Q	1705.426 35	2.140	47.1	278	0.321	0.0
	ACPF-DKH2	1705.424 65	2.136	46.8	282	0.956	0.0
	RCCSD(T)-DKH2	1705.416 93	2.090	42.1	313	0.351	0.0
	C-RCCSD(T)	1697.528 26	1.954	54.4	343	-2.49	0.0
	C-RCCSD(T)-DKH2	1706.193 78	1.981	53.2	356	2.60	0.0
	Expt.(D_0^0 , Ref. 12)				56.2		
$1^2\Delta_g$	MRCI+Q	1696.745 32	1.847	38.4	559	0.005	9.1
	ACPF	1696.743 79	1.847	37.9	554	-1.76	9.0
	RCCSD(T)	1696.737 51	1.808	34.5	676	-6.58	7.9
	MRCI-DKH2+Q	1705.405 09	1.851	33.7	624	15.4	13.3
	ACPF-DKH2	1705.403 35	1.853	33.5	594	0.205	13.4
	RCCSD(T)-DKH2	1705.396 78	1.815	29.4	690	5.14	12.6
	C-RCCSD(T)	1697.526 94	1.766	53.6	774	-0.656	0.83
	C-RCCSD(T)-DKH2	1706.184 84	1.768	47.6	768	-2.121	5.6

obtained through the RCCSD(T) method to the latter value we obtain $D_0^0 = 59.1(58.8) - \omega_e/2 = 58.6(58.3)$ kcal/mol, perhaps slightly overestimated. Core effects reduce the bond distance by $\delta r_e = 0.123$ Å at the RCCSD(T) level, therefore $r_e(\text{MRCI-DKH2+Q}) - \delta r_e = 2.140 - 0.123 = 2.017$ Å as contrasted to the C-RCCSD(T)-DKH2 value of 1.981 Å.

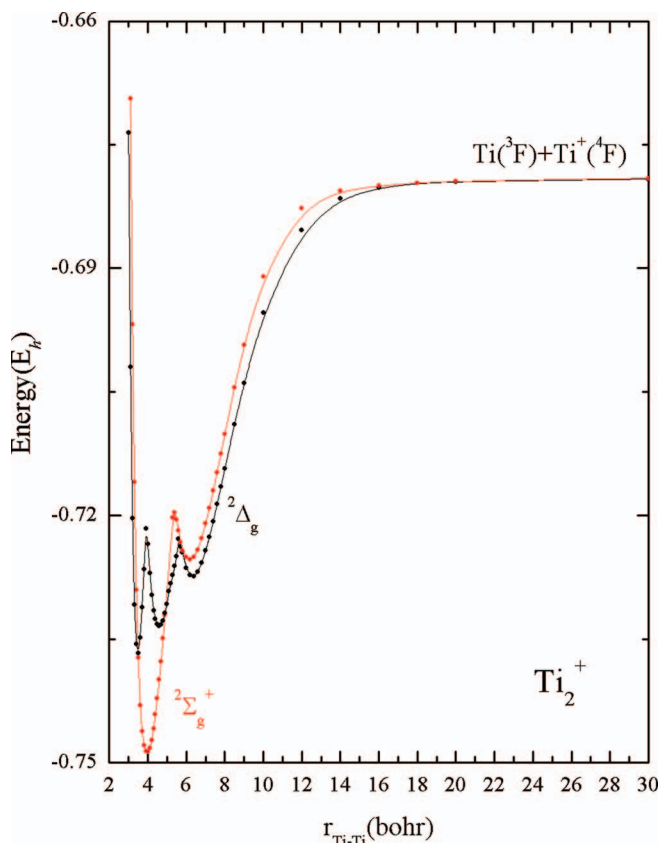


FIG. 3. MRCI/Qz PECs of 2 states of Ti_2^+ . Energies have been shifted by $+1696.0 E_h$.

Our recommended bond distance is $r_e = (2.017 + 1.981)/2 = 2.00$ Å. The experimental IE of Ti_2 is 5.93 ± 0.19 eV,¹² in acceptable agreement with the C-RCCSD(T)-DKH2 result of 5.64 eV.

For the $2^2\Delta_g$ state, taking into consideration the $3s^23p^6$ core effects at the CC level, the recommended bond distance is $r_e = r_e(\text{MRCI-DKH2+Q}) + \delta r_e = 1.851 - 0.042 = 1.81$ Å, as compared to 1.77 Å at the C-RCCSD(T)-DKH2 level. According to Table III the C-RCCSD(T)-DKH2 $T_e = 5.6$ kcal/mol is in agreement with the MRCI-DKH2+Q value after the inclusion of the subvalence core effects at the CC level, $T_e = 13.3 - 7.1 = 6.2$ kcal/mol.

V. FINAL REMARKS

Using MRCI and single reference CC methods combined with large basis sets, we have studied the electronic structure of Ti_2 and Ti_2^+ . In particular, we have constructed (valence) MRCI+Q PECs for 30 (Ti_2) and 2 (Ti_2^+) states, whereas for the lowest 4 states of Ti_2 and the 2 states of Ti_2^+ , scalar relativistic and subvalence ($3s^23p^6$) core correlation effects have been taken into account. We have to confess, however, that although our calculations are the best and most systematic so far in the literature, the results cannot be deemed as satisfactory, in other words do not reflect our strenuous efforts put in this project. As already stated, the almost insurmountable computational and conceptual difficulties of the $3d-M_2$ systems are due to the extremely dense manifold of the $\Lambda-\Sigma$ states.

The ground state of Ti_2 was considered to be up to now, rather “traditionally,” of the $3^3\Delta_g$ symmetry; the present calculations, although do not prove, suggest as well that this is very probably true. Recommended “best” theoretical bond distance and dissociation energy for the $X^3\Delta_g$ state are (experimental values in parenthesis), $r_e = 1.942$ ($r_0 = 1.9422 \pm 0.0008$) Å (Ref. 10) and $D_0^0 = 29.0$ (35.5 ± 4.4) kcal/mol (Ref. 12). Formally, the two Ti atoms are held together by one

and a half σ and two π bonds. Our calculations indicate, but again do not prove, that the first excited state, $1^1\Sigma_g^+$, is within 1 kcal/mol of the $X^3\Delta_g$ state.

By removing the symmetry defining d_δ electron from the $X^3\Delta_g$ state of Ti_2 , the $X^2\Sigma_g^+$ state of Ti_2^+ is obtained, with the first excited state of $^2\Delta_g$ symmetry about 6 kcal/mol higher.

Finally, in addition to the first four states of Ti_2 more thoroughly calculated, numerical results of quasi-quantitative accuracy for 26 higher states are also given. We believe that the present study is a step towards a better understanding of the electronic structure of Ti_2 , and of some use to the scientific community.

- ¹D. Tzeli, U. Miranda, I. G. Kaplan, and A. Mavridis, *J. Chem. Phys.* **129**, 154310 (2008).
²A. Kalemos, I. G. Kaplan, and A. Mavridis, *J. Chem. Phys.* **132**, 024309 (2010).
³A. Kant and B. Strauss, *J. Chem. Phys.* **41**, 3806 (1964).
⁴L. Pauling, *J. Am. Chem. Soc.* **69**, 542 (1947).
⁵A. Kant and S.-S. Lin, *J. Chem. Phys.* **51**, 1644 (1969).
⁶C. Cossé, M. Fouassier, T. Mejean, M. Tranquille, D. P. DiLella, and M. Moskovits, *J. Chem. Phys.* **73**, 6076 (1980).
⁷K. D. Bier, T. L. Haslett, A. D. Kirkwood, and M. Moskovits, *Faraday Discuss. Chem. Soc.* **86**, 181 (1988).
⁸T. L. Haslett, M. Moskovits, and A. L. Weitzman, *J. Mol. Spectrosc.* **135**, 259 (1989).
⁹C. W. Bauschlicher, Jr., H. Partridge, S. R. Langhoff, and M. Rosi, *J. Chem. Phys.* **95**, 1057 (1991).
¹⁰M. Doverstål, B. Lindgren, U. Sassenberg, C. A. Arrington, and M. D. Morse, *J. Chem. Phys.* **97**, 7087 (1992).
¹¹L. Lian, C.-X. Su, and P. B. Armentrout, *J. Chem. Phys.* **97**, 4084 (1992).
¹²L. M. Russon, S. A. Heidecke, M. K. Birke, J. Conceicao, M. D. Morse, and P. B. Armentrout, *J. Chem. Phys.* **100**, 4747 (1994).
¹³M. Doverstål, L. Karlsson, B. Lindgren, and U. Sassenberg, *Chem. Phys. Lett.* **270**, 273 (1997).
¹⁴H.-J. Himmel and A. Bihlmeir, *Chem. Eur. J.* **10**, 627 (2004).
¹⁵O. Hübner, H.-J. Himmel, L. Manceron, and W. Klopper, *J. Chem. Phys.* **121**, 7195 (2004).

- ¹⁶A. Wolf and H.-H. Schmidtke, *Int. J. Quantum Chem.* **18**, 1187 (1980).
¹⁷S. P. Walch and C. W. Bauschlicher, Jr., "Comparison of *Ab Initio Quantum Chemistry with Experiment for Small Molecules*," edited by R. J. Bartlett (D. Reidel, Dordrecht, Holland, 1985).
¹⁸Y.-I. Suzuki, T. Noro, F. Sasaki, and H. Tatewaki, *J. Mol. Struct.: THEOCHEM* **461**, 351 (1990).
¹⁹(a) J. Harris and R. O. Jones, *J. Chem. Phys.* **70**, 830 (1979); (b) V. D. Fursova, A. P. Klyagina, A. A. Levin, and G. L. Gutsev, *Chem. Phys. Lett.* **116**, 317 (1985); (c) R. Bergström, A. S. Lunell, and L. A. Eriksson, *Int. J. Quantum Chem.* **59**, 427 (1996); (d) S. Yanagisawa, T. Tsuneda, and K. Hirao, *J. Chem. Phys.* **112**, 545 (2000); (e) C. J. Barden, J. C. Rienstra-Kiracofe, and H. F. Schaefer III, *J. Chem. Phys.* **113**, 690 (2000); (f) S. H. Wei, Z. Zeng, J. Q. You, X. H. Yan, and X. G. Gong, *ibid.* **113**, 11127 (2000); (g) G. L. Gutsev and C. W. Bauschlicher, Jr., *J. Phys. Chem. A* **107**, 4755 (2003); (h) M. Valiev, E. J. Bylaska, and J. H. Weare, *J. Chem. Phys.* **119**, 5955 (2003); (i) F. Furche and J. P. Perdew, *ibid.* **124**, 044103 (2006); (j) M. Salazar-Villanueva, P. H. Hernández Tejada, U. Pal, J. F. Rivas-Silva, J. I. Rodríguez Mora, and J. A. Ascencio, *J. Phys. Chem. A* **110**, 10274 (2006); (k) Y. Zhao and D. G. Truhlar, *J. Chem. Phys.* **124**, 224105 (2006).
²⁰N. Balabanov and K. A. Peterson, *J. Chem. Phys.* **123**, 064107 (2005).
²¹N. Douglas and N. M. Kroll, *Ann. Phys.* **82**, 89 (1974).
²²B. A. Hess, *Phys. Rev. A* **32**, 756 (1985); *ibid.* **33**, 3742 (1986).
²³W. A. de Jong, R. J. Harrison, and D. A. Dixon, *J. Chem. Phys.* **114**, 48 (2001).
²⁴R. J. Gdanitz and R. Ahlrichs, *Chem. Phys. Lett.* **143**, 413 (1988); H.-J. Werner and P. J. Knowles, *Theor. Chim. Acta* **78**, 175 (1990).
²⁵K. Raghavachari, G. W. Trucks, J. A. Pople, and M. Head-Gordon, *Chem. Phys. Lett.* **157**, 479 (1989); J. D. Watts and R. J. Bartlett, *J. Chem. Phys.* **98**, 8718 (1993); P. J. Knowles, C. Hampel, and H.-J. Werner, *ibid.* **99**, 5219 (1993); **112**, 3106E (2000).
²⁶H.-J. Werner and P. J. Knowles, *J. Chem. Phys.* **89**, 5803 (1988); P. J. Knowles and H.-J. Werner, *Chem. Phys. Lett.* **145**, 514 (1988).
²⁷S. R. Langhoff and E. R. Davidson, *Int. J. Quantum Chem.* **8**, 61 (1974); E. R. Davidson and D. W. Silver, *Chem. Phys. Lett.* **52**, 403 (1977).
²⁸H.-J. Werner, P. J. Knowles, F. R. Manby, M. Schütz *et al.*, Molpro, version 2010.1, a package of *ab initio* programs, 2010, see <http://www.molpro.net>.
²⁹Y. Ralchenko, A. E. Kramida, J. Reader, and NIST ASD Team (2010). *NIST Atomic Spectra Database* (National Institute of Standards and Technology, Gaithersburg, MD, 2010); see <http://physics.nist.gov/asd>.
³⁰C. F. Bunge, J. A. Barrientos, and A. V. Bunge, *At. Data Nucl. Data Tables* **53**, 113 (1993).